Physics Letters A 418 (2021) 127709

Contents lists available at ScienceDirect

Physics Letters A

www.elsevier.com/locate/pla

Investigation of uniaxial strain in twisted few-layer MoS_2

Weibin Zhang [a], Fanghua Cheng [b], Junwei Huang [b,*], Hongtao Yuan [b], Quan Wang [a,*]

[a] Zhenjiang Key Laboratory of Advanced Sensing Materials and Devices, School of Mechanical Engineering, Jiangsu University, Zhenjiang 212013, PR China
[b] College of Engineering and Applied Sciences, National Laboratory of Solid State Microstructures, and Jiangsu Key Laboratory of Artificial Functional Materials, Nanjing University, Nanjing 210000, PR China

ARTICLE INFO

Article history:
Received 2 August 2021
Received in revised form 4 September 2021
Accepted 20 September 2021
Available online 22 September 2021
Communicated by J.G. Lu

Keywords:
MoS_2
Few-layer
Interlayer twisted
Photoluminescence
Raman spectroscopy

ABSTRACT

Applying strain is an effective way to change the optical properties of two-dimensional (2D) materials like molybdenum disulfide (MoS_2). In this work, the technical details were provided to perform uniaxial strain measurements in the range of 0∼5% in twisted monolayer-monolayer MoS_2 (tMMM), twisted monolayer-bilayer MoS_2 (tMBM), twisted bilayer-monolayer MoS_2 (tBMM) and twisted bilayer-bilayer MoS_2 (tBBM). The redshift and splitting of the $E_{2g}{}^1$ peak in twisted few-layer MoS_2 with increased strain are found by Raman spectroscopy and a Grüneisen parameter of ∼1.31 is extracted. The decrease of optical band gap in MoS_2 was measured by photoluminescence (PL) spectroscopy, and it changes approximately linear with strain, which is −16.27 meV/% strain for tMMM and −14.19 meV/% strain for tBBM. The intensity of A peak in PL spectra decreases to one third of its original value with an applied strain of ∼5% for the twisted angle around 11°. However, twisted few-layer MoS_2 exhibits strain relaxation at higher strain. This relaxation causes the bandgap to cease further redshift. The findings in this paper can help to better understand the effects of strain on the optical properties in twisted few-layer MoS_2, and is applicable to other 2D materials.

1. Introduction

Strain engineering has been proved to be an effective method to adjust the properties of 2D materials [1]. There are no dangling bonds on the surface of 2D materials, so they have strong elasticity to mechanical deformation, which makes it possible to adjust their performance in large strain range. Before rupturing due to strain, 2D materials can withstand a deformation by an order of magnitude larger than their bulk materials [1]. The breaking point during strain engineering is only determined by the inherent strength of the atomic bonds in the 2D materials. Due to these characteristics, strain engineering experiments can be applied to 2D materials, and have promote several works in the past few years [2–4].

MoS_2 has attracted the interest of many experts due to its unique physical properties [5–10]. From bulk to monolayer, the PL emission of monolayer MoS_2 is enhanced by more than 10^4-fold since MoS_2 undergoes a bandgap transition from indirect to direct [11,12]. Optoelectronic has a wide range of applications [13,14] including light-emitting devices, solar cells, and photodetectors, by the PL emission plays an important role. Therefore, it is of great significance to controllably tuning the PL properties of MoS_2 [15,16]. Due to the associated changes of interlayer coupling, [17] the PL properties of MoS_2 vary with both the number of layers and the distance between layers [18]. Thus, controlling the interlayer coupling of MoS_2 can effectively modulate its electronic and optical properties.

In electronics, applying strain to modify the band structure of 2D materials is a common strategy to tune the performance of a device. Although monolayer MoS_2 has shown outstanding results in flexible electronics [19], few-layer MoS_2 also has some characteristics. In some cases, few-layer MoS_2 may be more suitable for large-scale applications. Previous studies mainly focused on the optical properties of monolayer MoS_2 under strain [20], the effects of strain on twisted few-layer MoS_2 are not well understood. In this paper, Raman and PL spectra were used to shed light on how twisted monolayer-monolayer MoS_2 (tMMM), twisted monolayer-bilayer MoS_2 (tMBM), twisted bilayer-monolayer MoS_2 (tBMM) and twisted bilayer-bilayer MoS_2 (tBBM) are affected under uniaxial tensile strain.

2. Experimental

One large-area MoS_2 flake, containing monolayer (1L) and bilayer (2L), was mechanically peeled off from the bulk material onto a PDMS (dimethylsiloxane) substrate, and then transferred onto a

* Corresponding authors.
E-mail addresses: junweihuang@nju.edu.cn (J. Huang), wangq@ujs.edu.cn (Q. Wang).

https://doi.org/10.1016/j.physleta.2021.127709
0375-9601/

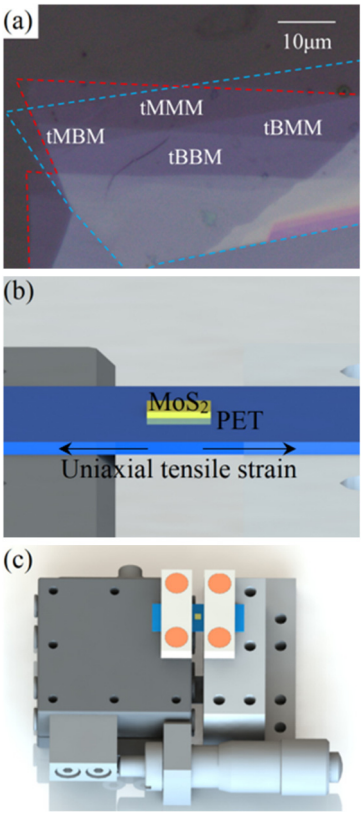

Fig. 1. Sample preparation and the experimental method. (a) Picture of twisted few-layer MoS_2 samples with twisted angle of 11°. The blue (red) lines in (a) outline the bottom (top) layer of twisted few-layer MoS_2. (b) Schematic depiction of the uniaxial tensile strain experiment. (c) Self-made linear displacement setup for uniaxial tensile strain experiments on 2D materials. (For interpretation of the colors in the figure(s), the reader is referred to the web version of this article.)

flexible PET (ethylene terephthalate) substrate (150 μm in thickness). The layer number of MoS_2 was verified by Raman spectra. Another large-area MoS_2 flake (also containing 1L and 2L) was directly stacked onto the former one with a twisted angle of 11° by using a dry-transfer method. As shown in Fig. 1a, this twisted MoS_2 sample possesses four stacking sequences, namely tMMM, tMBM, tBMM, and tBBM.

To investigate the effect of strain on the optical properties of this twisted MoS_2 sample, we developed a single-axis translation stage with side-mounted micrometer to provide a controllable uniaxial tensile strain passing through the PET substrate, as presented in Figs. 1b and 1c. For our home-made stain stage, the initial distance between the left movable part and the right fixed one was set to be 2000 μm. The PET substrate with MoS_2 samples was placed on the platform (note that the samples should be suspended in the middle), and clamped with spacers and bolts. The spiral micrometer (with an accuracy of 10 μm) was manually controlled to relatively move the left part, enabling to stretch the PET substrate and then apply a uniaxial tensile strain to the MoS_2 samples. The strain rate with an accuracy of ~0.5% was precisely obtained by measuring its high-resolution microscopic photographs. This method can provide a uniaxial tensile strain with a rate up to 5%, which is enough to investigate the evolution of the Raman and PL spectra in the twisted few-layer MoS_2. Raman and PL spectra measurements were performed using a confocal Raman microscopy system (WITec Alpha 300R). A 532 nm solid state laser with the average laser power ~150 μW was employed as the excitation source which did not damage our samples. The spectra were collected at room temperature using a ×50 objective lens on the sample plane and either a 1800 (Raman) or 150 (PL) g/mm grating.

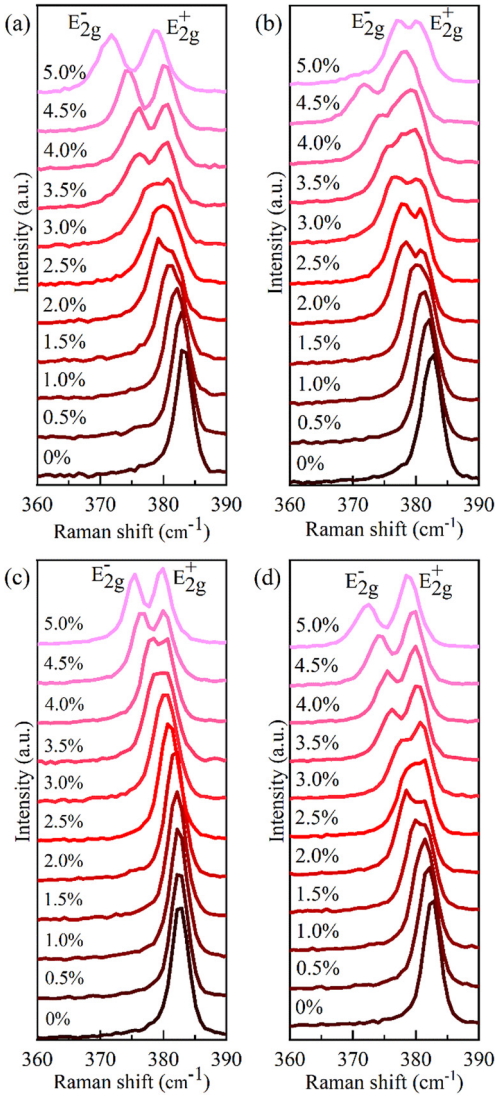

Fig. 2. Raman spectra of twisted few-layer MoS_2 with increasing strain. All the spectra are shifted vertically for clarity. (a) tMMM. (b) tMBM. (c) tBMM. (d) tBBM.

3. Results and discussion

Further, the strain dependence of the Raman spectra of twisted few-layer MoS_2 is studied. For the unstrained sample, as previously reported [21], the A_{1g} Raman mode at 403 cm^{-1} is associated to out-of-plane vibrations, while the doubly degenerate $E_{2g}{}^1$ Raman mode at 384 cm^{-1} is ascribed to in-plane vibrations. Fig. 2 displays the Raman spectra of this twisted few-layer MoS_2 sample under various uniaxial tensile strain. The prominent $E_{2g}{}^1$ Raman peaks redshifts with the strain increases, indicating the softening of the in-plane vibrational mode. Interestingly, the $E_{2g}{}^1$ mode for all four stacking sequences splits into doubly degenerated $E_{2g}{}^+$ and $E_{2g}{}^-$ modes with increasing strain. The uniaxial tensile strain deforms the lattice and destroys the crystal symmetry, resulting in the displacement of atoms out of their equilibrium locations and the change of phonon modes [22]. These two splitting $E_{2g}{}^+$ and $E_{2g}{}^-$ peaks correspond to in-plane atomic vibrations, which are perpendicular and parallel to the direction of applied strain, respectively. With the strain increases, the $E_{2g}{}^-$ peak keeps to shift towards lower Raman number, while the $E_{2g}{}^+$ peak shifts oppositely. Fig. 2 shows a significant red shift in the $E_{2g}{}^1$ ($E_{2g}{}^+$ and $E_{2g}{}^-$) peak. The continuous movement of the $E_{2g}{}^+$ and $E_{2g}{}^-$ modes indicates that there is no detectable slip between the PET substrate and MoS_2

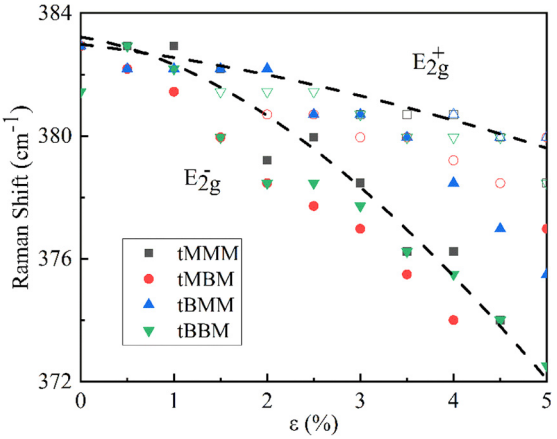

Fig. 3. Phonon frequencies of MoS_2 as a function of uniaxial tensile strain. The peak location of the $E_{2g}{}^{+}$ and $E_{2g}{}^{-}$ Raman modes, extracted by fitting the peaks to a Lorentzian, as their degeneracy is broken by straining MoS_2. Different colors represent individual layers. The hollow data points represent $E_{2g}{}^{+}$. The black dashed line is a Lorenz fit of tMMM.

Table 1
Summary of the experimental gauge factors for the different phonon shifts, the Grüneisen parameters and the shear deformation potential measured or calculated in tMMM, tMBM, tBMM and tBBM.

Samples	Gauge factor (cm^{-1}/%)		$\gamma_{E'}$	$\beta_{E'}$
	$E_{2g}{}^{-}$	$E_{2g}{}^{+}$		
tMMM	−2.03	−0.81	1.31	0.54
tMBM	−1.13	−0.56	0.65	0.45
tBMM	−1.42	−0.56	0.59	0.60
tBBM	−1.62	−0.54	0.67	0.30

sample within the applied uniaxial tensile strain range. The abnormal blue shift of the $E_{2g}{}^{-}$ peak in tMBM (Fig. 2b) may be caused by strain relaxation.

Fig. 3 shows the correlation between the shift of the $E_{2g}{}^{1}$ Raman mode and the strain. It is found that, for tMMM, the $E_{2g}{}^{-}$ peak shifts by −2.03 cm^{-1}/% strain, while the $E_{2g}{}^{+}$ peak shifts by −0.81 cm^{-1}/% strain, in similarity with results obtained by *Rice et al.* applying uniform uniaxial strain to MoS_2. The peak shifts corresponding to the other three sequences are smaller than that of tMMM, and the values are summarized in Table 1. For the strain range of 0∼5%, the peak positions of tMMM, tBMM and tBBM samples move at a similar rate and there is no hysteresis during multiple loading/unloading cycles, which indicates that the MoS_2 samples do not produce a large number of defects. The tMBM sample behaves similarly but fails when the strain reaches 5%.

The parameters characterizing anharmonicity of molecular potentials [23]: the Grüneisen parameter γ and the shear deformation potential β can be calculated based on the strain dependence of the $E_{2g}{}^{1}$ Raman mode.

$$\gamma_{E'} = -\frac{\Delta\omega_{E^{+}_{2g}} + \Delta\omega_{E^{-}_{2g}}}{2\omega_{E^{1}_{2g}}(1-\nu)\varepsilon} \tag{1}$$

$$\beta_{E'} = \frac{\Delta\omega_{E^{+}_{2g}} - \Delta\omega_{E^{-}_{2g}}}{\omega_{E^{1}_{2g}}(1+\nu)\varepsilon} \tag{2}$$

Here, ω is the frequency of the Raman mode, $\Delta\omega$ is the change of frequency per unit strain, ε is the induced strain of samples, and ν is Poisson's ratio. For the material attached to the substrate, its Poisson's ratio is the Poisson ratio of the substrate, which is 0.33. The tMMM yields a Grüneisen parameter of 1.31, which is obviously less than that of graphene (1.99) and comparable that of

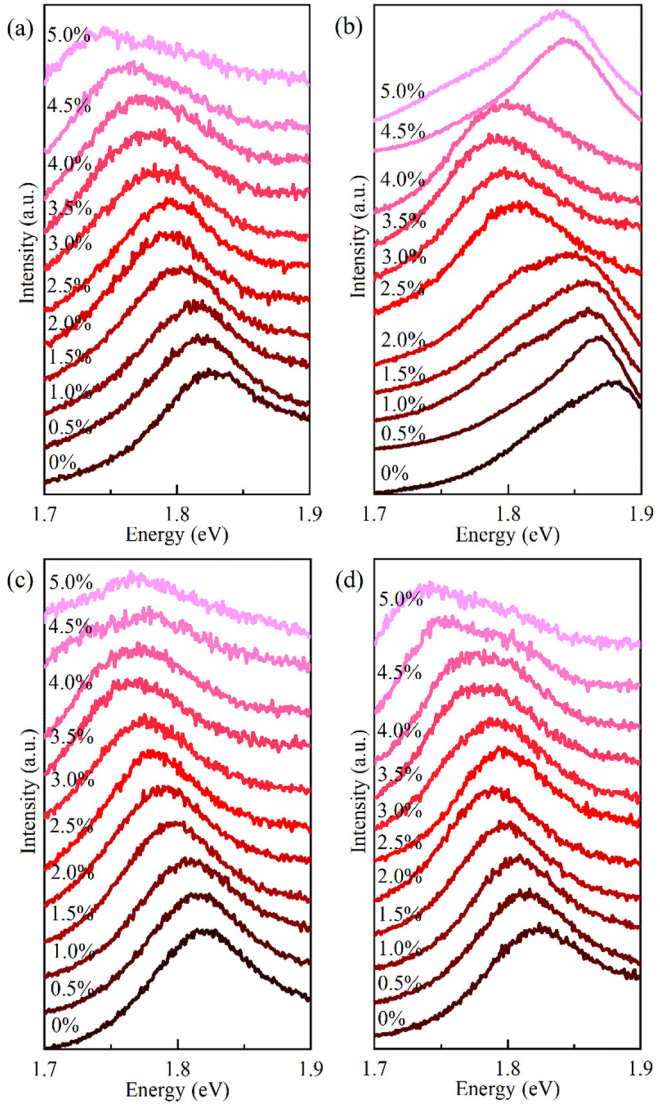

Fig. 4. Photoluminescence spectra of twisted few-layer MoS_2 with increasing strain. All the spectra are shifted vertically for clarity. (a) tMMM. (b) tMBM. (c) tBMM. (d) tBBM.

hexagonal boron nitride (0.95∼1.2) [24–26]. The calculation results are summarized in Table 1. The Grüneisen parameter contains almost all the information of the equation of state and is of great significance to study the thermodynamic properties, elasticity and anharmonicity of matter. The calculation of the Grüneisen parameter and shear deformation potential can help to further understand the properties of twisted few-layer MoS_2.

The evolution of the band structure in the twisted few-layer MoS_2 with uniaxial tensile strain was investigated by PL spectroscopy. MoS_2 (3–5 layers thick) is an indirect bandgap semiconductor with the exciton binding energy of about 100 meV. Previous studies of 0–2.5% buckling-induced strain have shown that the PL spectrum of few-layer MoS_2 is mainly controlled by the direct gap transitions at the K point of the Brillouin zone between the valence band and the conduction band, so it should not be significantly influenced by the applied strain [27]. However, we applied a uniaxial tensile strain in the range of 0–5% to few-layer MoS_2 and obtained different results.

Fig. 4 shows the evolution of PL spectra in twisted few-layer MoS_2 with applying strain from 0% to 5%. With the strain increases, almost all the PL peaks show a redshift. The observed PL peak shift is mainly attributed to the change of single-particle bandgap, be-

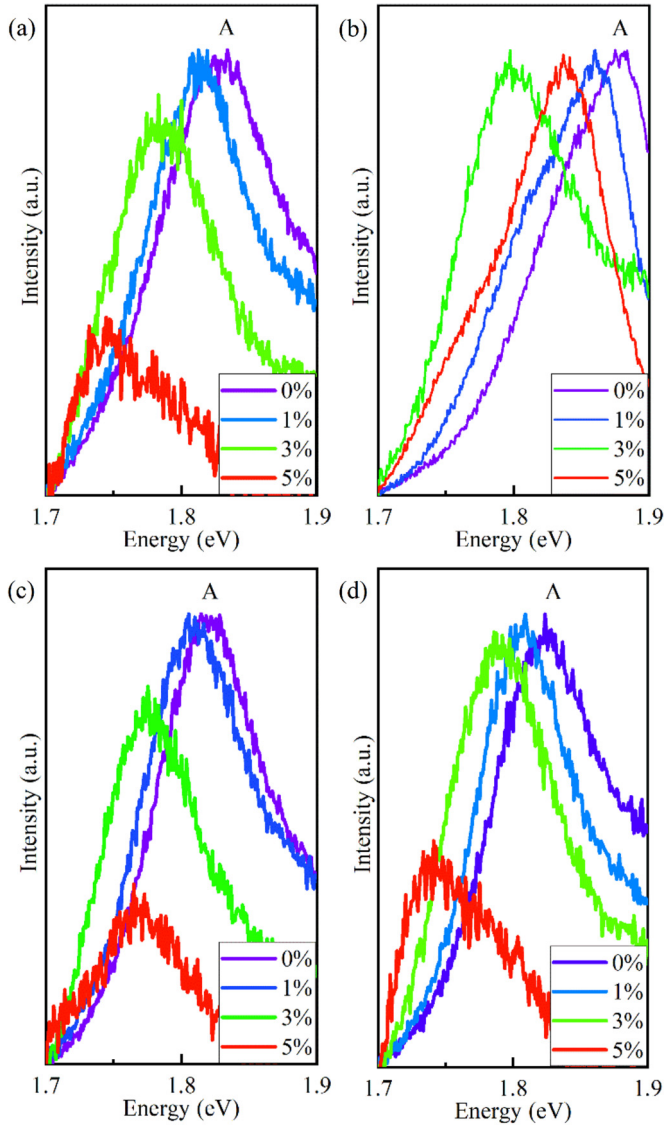

Fig. 5. Photoluminescence spectra of strained twisted few-layer MoS_2 at $\varepsilon = 0$, 1, 3, 5%. All the spectra are shifted vertically for clarity. (a) tMMM. (b) tMBM. (c) tBMM. (d) tBBM.

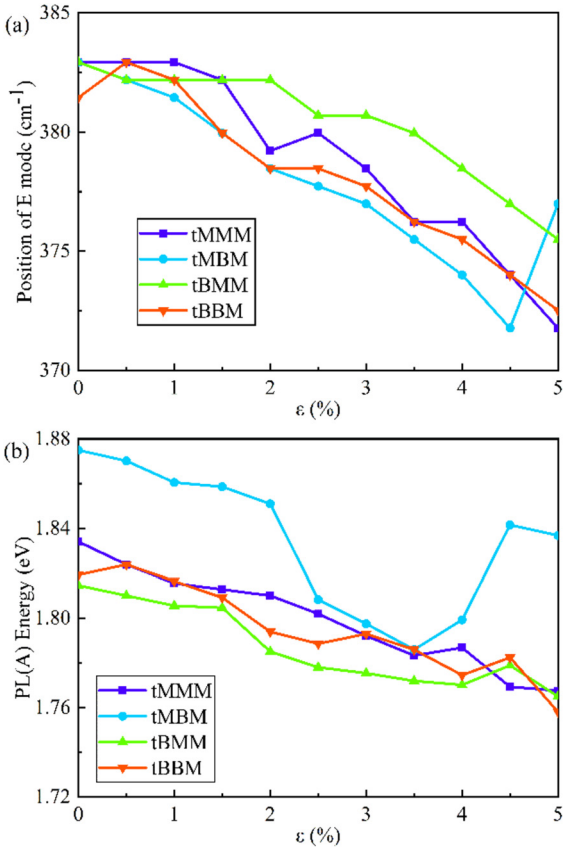

Fig. 6. Strain study on twisted few-layer MoS_2. (a) The position of E Raman mode. (b) The PL A-exciton energy.

cause both theory and experiment have proved that the change of the exciton binding energy under strain is negligible [27–29]. Lorentzian function was used to fit the spectra and determine the position and intensity of the PL peaks, in which the main peak is labeled as A peak. For all measured twisted few-layer MoS_2 samples, the A peak shows an approximately linear redshift with the strain, at a rate of −16.27 meV/% strain for tMMM, −8.61 meV/% strain for tBMM and −14.19 meV/% strain for tBBM. While the intensity of the A peak in the above three samples decreases to one third of their initial values with an applied strain of ∼5%, as shown in Fig. 5. Previous studies claimed that the A peak strength of bilayer MoS_2 is independent of strain because the strain is too small (only 2%). Under a high strain level, flakes may develop wrinkles or cracks to relax the strain [30]. Strain relaxation is formed at high strain level to partially resist the further increase of internal tensile strain of MoS_2, which finally leads to end of bandgap redshift. As for the reason why the strain relaxation phenomenon only appears in tMBM sample but not in the other three samples, it is considered that it may be due to the influence of residual glue from PDMS.

The frequency of the in-plane E_{2g} mode (ω_E) and the A-exciton energy (referred to as PL(A)) as a function of the applied strain are shown in Fig. 6. As previously reported, both ω_E and PL(A) display a monotonic decrease as a function of strain for MoS_2 with different thicknesses. In comparison, by applying ∼5% uniaxial strain, the change is more dramatic for twisted few-layer MoS_2, whose frequencies shift over 10 cm^{-1}. Except this special case, the ω_E value decreases monotonously. This suggests that the interaction of the upper layers keeps the underneath area from slipping, while the marginal area is easier to relax. It is concluded that the observed slipping is localized between two layers.

The observed redshift of the PL peaks is indicative of strain-induced reduction of band gaps in twisted few-layer MoS_2. The observed change trend of the position and intensity of the PL peak relative to the applied strain is attributed to the decrease of the band gap and PL efficiency caused by strain, because the change in the PL can in principle be regarded as an indicator that the electronic band structure by the applied strain, which is consistent with the theoretical prediction [31]. Therefore, the optical and vibrational characteristics of the twisted few-layer MoS_2 flake changes significant under the application of strain, which indicates that the strain engineering experimental design is appropriate.

The Raman peak shift rate of tMMM is the fastest, which is due to the more obvious phonon softening of the twisted bilayer MoS_2. The PL intensity of tBBM does not decrease significantly when the applied strain is less than 4%. The optical properties of thicker MoS_2 flakes require greater applied strain to tune. The optical performance tuning results of tMBM and tBMM are between the above two. Since the bottom layer of tMBM is a monolayer layer flake and the top layer is a bilayer flake, the structure is unstable. Therefore, strain relaxation is more likely to occur in tMBM rather than tBMM.

4. Conclusions

In summary, we developed a linear displacement setup suitable for strain-controlled spectra experiments in 2D materials, and performed a wide range of uniaxial tensile strain on the optical properties in the twisted few-layer MoS_2. When strain breaks the symmetry of the crystal, the double degenerate $E_{2g}{}^1$ Raman peak splits into two subpeaks under the application of strain. The A PL peak redshifts approximate linearly with the strain, and its intensity decreases to one third of its original value when the applied strain is ∼5%, which indicates that the MoS_2 can adhere to the flexible substrate well after transfer. However, a relative sliding between the layers under a large strain is also observed, which leads to a hysteresis of the Raman and PL spectra upon further application of strain. The complex force condition at the edge makes this interlayer sliding more likely to occur. The results of this paper are believed to provide a better understanding in the effects of strain engineering in twisted MoS_2 and should also be applied to other 2D TMDCs.

CRediT authorship contribution statement

Weibin Zhang: Data curation, Writing – original draft preparation.

Fanghua Cheng: Verification, Conducting a research and investigation process.

Junwei Huang: Development or design of methodology, Creation of models.

Hongtao Yuan: Ideas, Formulation of overarching research goals and aims.

Quan Wang: Supervision, Writing – reviewing & editing.

All the authors contributed to discussions.

Declaration of competing interest

The authors declare that they have no known competing financial interests or personal relationships that could have appeared to influence the work reported in this paper.

Acknowledgements

This work is supported by the National Natural Science Foundation of China (No. 51675246, 52072168, 51861145201, 91750101, 21733001), the National Key Basic Research Program of the Ministry of Science and Technology of China (2018YFA0306200), the Fundamental Research Funds for the Central Universities (021314380078, 021314380104, 021314380147).

References

[1] R. Roldán, A. Castellanos-Gomez, E. Cappelluti, F. Guinea, Strain engineering in semiconducting two-dimensional crystals, J. Phys. Condens. Matter 27 (2015) 313201.
[2] K.L. He, C. Poole, K.F. Mak, J. Shan, Experimental demonstration of continuous electronic structure tuning via strain in atomically thin MoS_2, Nano Lett. 13 (2013) 2931–2936.
[3] Y.Y. Hui, X.F. Liu, W.J. Jie, N.Y. Chan, J.H. Hao, Y.T. Hsu, L.J. Li, W.L. Guo, S.P. Lau, Exceptional tunability of band energy in a compressively strained trilayer MoS_2 sheet, ACS Nano 7 (2013) 7126–7131.
[4] D. Lloyd, X.H. Liu, J.W. Christopher, L. Cantley, A. Wadehra, B.L. Kim, B.B. Goldberg, A.K. Swan, J.S. Bunch, Band gap engineering with ultralarge biaxial strains in suspended monolayer MoS_2, Nano Lett. 16 (2016) 5836–5841.
[5] A. Ramasubramaniam, Large excitonic effects in monolayers of molybdenum and tungsten dichalcogenides, Phys. Rev. B 86 (2012) 115409.
[6] H.N. Wang, C.J. Zhang, W.M. Chan, S. Tiwari, F. Rana, Ultrafast response of monolayer molybdenum disulfide photodetectors, Nat. Commun. 6 (2015) 8831.
[7] D. Jariwala, V.K. Sangwan, D.J. Late, J.E. Johns, V.P. Dravid, T.J. Marks, L.J. Lauhon, M.C. Hersam, Band-like transport in high mobility unencapsulated single-layer MoS_2 transistors, Appl. Phys. Lett. 102 (2013) 173107.
[8] K.F. Mak, K.L. Mcgill, J. Park, P.L. Mceuen, The valley Hall effect in MoS_2 transistors, Science 344 (2014) 1489–1492.
[9] S. Sahoo, A.P.S. Gaur, M. Ahmadi, J.F. Guinel, R.S. Katiyar, Temperature-dependent Raman studies and thermal conductivity of few-layer MoS_2, Physics 117 (2013) 9042–9047.
[10] X. Liu, G. Zhang, Q.X. Pei, Y.W. Zhang, Phonon thermal conductivity of monolayer MoS_2 sheet and nanoribbons, Appl. Phys. Lett. 103 (2013) 133113.
[11] K.F. Mak, C. Lee, J. Hone, J. Shan, T.F. Heinz, Atomically thin MoS_2: a new direct-gap semiconductor, Phys. Rev. Lett. 105 (2010) 136805.
[12] A. Splendiani, L. Sun, Y.B. Zhang, T.S. Li, J. Kim, C.Y. Chim, G. Galli, F. Wang, Emerging photoluminescence in monolayer MoS_2, Nano Lett. 10 (2010) 1271–1275.
[13] K. Wei, T. Jiang, Z.J. Xu, J.H. Zhou, J. You, Y.X. Tang, H. Li, R.Z. Chen, X. Zheng, S.S. Wang, K. Yin, Z.Y. Wang, J. Wang, X.G. Cheng, Ultrafast carrier transfer promoted by interlayer Coulomb coupling in 2D/3D perovskite heterostructures, Laser Photonics Rev. 12 (2018) 1800128.
[14] K. Wei, Z. Xu, R. Chen, X. Zheng, X. Cheng, T. Jiang, Temperature-dependent excitonic photoluminescence excited by two-photon absorption in perovskite $CsPbBr_3$ quantum dots, Opt. Lett. 41 (2016) 3821–3824.
[15] S. Mouri, Y. Miyauchi, K. Matsuda, Tunable photoluminescence of monolayer MoS_2 via chemical doping, Nano Lett. 13 (2013) 5944–5948.
[16] D.W. Li, Q.M. Zou, X. Huang, H.R. Golgir, K. Keramatnejad, J.F. Song, Z.Y. Xiao, L.S. Fan, X. Hong, L. Jiang, J.F. Silvain, S. Sun, Y.F. Lu, Controlled defect creation and removal in graphene and MoS_2 monolayers, Nanoscale 9 (2017) 8997–9008.
[17] P.C. Yeh, W. Jin, N. Zaki, J. Kunstmann, D.A. Chenet, G. Arefe, J.T. Sadowski, J.I. Dadap, P. Sutter, J.C. Hone, Direct measurement of the tunable electronic structure of bilayer MoS_2 by interlayer twist, Nano Lett. 16 (2016) 953–959.
[18] C. Lee, H. Yan, L.E. Brus, T.F. Heinz, J. Hone, S. Ryu, Anomalous lattice vibrations of single- and few-layer MoS_2, ACS Nano 4 (2010) 2695–2700.
[19] M. Amani, R.A. Burke, R.M. Proie, M. Dubey, Nanotechnology 26 (2015) 115202.
[20] C. Rice, R.J. Young, R. Zan, U. Bangert, D. Wolverson, T. Georgiou, R. Jalil, K.S. Novoselov, Raman-scattering measurements and first-principles calculations of strain-induced phonon shifts in monolayer MoS_2, Phys. Rev. B 87 (2013) 081307.
[21] H. Li, Q. Zhang, C.C.R. Yap, B.K. Tay, T.H.T. Edwin, A. Olivier, D. Baillargeat, From bulk to monolayer MoS_2: evolution of Raman scattering, Adv. Funct. Mater. 22 (2012) 1385–1390.
[22] W. Wu, J. Wang, P. Ercius, N.C. Wright, D.M. Leppert-Simenauer, R.A. Burke, M. Dubey, A.M. Dogare, M.T. Pettes, Giant mechano-optoelectronic effect in an atomically thin semiconductor, Nano Lett. 18 (2018) 2351–2357.
[23] H.J. Conley, B. Wang, J.I. Ziegler, R.F. Haglund, S.T. Pantelides, K.I. Bolotin, Bandgap engineering of strained monolayer and bilayer MoS_2, Nano Lett. 13 (2013) 3626–3630.
[24] T.M.G. Mohiuddin, A. Lombardo, R.R. Nair, A. Bonetti, G. Savini, R. Jalil, N. Bonini, D.M. Basko, C. Galiotis, N. Marzari, K.S. Novoselov, A.K. Geim, A.C. Ferrari, Uniaxial strain in graphene by Raman spectroscopy: G peak splitting, Gruneisen parameters, and sample orientation, Phys. Rev. B 79 (2009) 205433.
[25] G. Kern, G. Kresse, J. Hafner, Ab initio calculation of the lattice dynamics and phase diagram of boron nitride, Phys. Rev. B 59 (1999) 8551–8559.
[26] J.A. Sanjurjo, E. López-Cruz, P. Vogl, M. Cardona, Dependence on volume of the phonon frequencies and their effective charges of several III-V semiconductors, Phys. Rev. B 28 (1983) 4579–4584.
[27] A. Castellanos-Gomez, R. Roldán, E. Cappelluti, M. Buscema, F. Guinea, H.S.J. van der Zant, G.A. Steele, Local strain engineering in atomically thin MoS_2, Nano Lett. 13 (2013) 5361–5366.
[28] H.L. Shi, H. Pan, Y.W. Zhang, B.I. Yakobson, Strong ferromagnetism in hydrogenated monolayer MoS_2 tuned by strain, Phys. Rev. B 88 (2013) 205305.
[29] J. Feng, X.F. Qian, C.W. Huang, J. Li, Strain-engineered artificial atom as a broad-spectrum solar energy funnel, Nat. Photonics 6 (2012) 865–871.
[30] Q.H. Zhang, Z.Y. Chang, G.Z. Xu, Z.Y. Wang, Y.P. Zhang, Z.Q. Xu, S.J. Chen, Q.L. Bao, J.Z. Liu, Y.W. Mai, W.H. Duan, M.S. Fuhrer, C.X. Zheng, Strain relaxation of monolayer WS_2 on plastic substrate, Adv. Funct. Mater. 26 (2016) 8707–8714.
[31] S. Pak, J. Lee, A. Jang, S. Kim, K. Park, J.I. Sohn, S. Cha, Strain-engineering of contact energy barriers and photoresponse behaviors in monolayer MoS2 flexible devices, Adv. Funct. Mater. 30 (2020) 2002023.